



Diatoms as paleoproductivity proxy in the NW Iberian coastal upwelling system (NE Atlantic)

Diana Zúñiga^{1,2}, Celia Santos^{3,4}, María Froján², Emilia Salgueiro^{3,5}, Marta M. Rufino^{3,5}, Francisco De la Granda⁶, Francisco G. Figueiras², Carmen G. Castro², Fátima Abrantes^{3,5}

5

¹ University of Vigo, Applied Physics Department, Campus Lagoas Marcosende, E-36310, Vigo, Spain

² Consejo Superior de Investigaciones Científicas (CSIC), Instituto de Investigaciones Marinas (IIM), E-36208, Vigo, Spain

³ Instituto Português do Mar e da Atmosfera (IPMA), Div. Geologia e Georecursos Marinhos, 1749-077, Lisbon, Portugal

⁴ MARUM, Center for Marine Environmental Sciences, Leobener Strasse, 28359, Bremen, Germany.

10 ⁵ CCMAR - Centre of Marine Sciences. Universidade do Algarve, Campus de Gambelas, 8005-139 Faro

⁶ Bundesamt für Seeschifffahrt und Hydrographie, Bernhard-Nocht-Str. 78, 20359, Hamburg, Germany

Correspondence to: Diana Zúñiga (diana.zuniga@uvigo.es; imissions@gmail.com)

Abstract. The objective of the current work is to better understand how diatoms species determine primary production signal in exported and buried particles. We evaluated how the diatom's abundance and assemblage composition is transferred from the photic zone into the seafloor sediments. A combined analysis of water column, sediment trap and surface sediment samples recovered in the NW Iberian coastal upwelling system was used.

15 Diatom fluxes ($2.2 \pm 5.6 \cdot 10^6 \# \text{ valves m}^{-2} \text{ d}^{-1}$) represented the majority of the siliceous microorganisms sinking out from the photic zone and showed strong seasonal variability. During downwelling seasons, diatoms export signal was strongly affected by resuspension of bottom sediments and intense Minho and Douro riverine inputs, with benthic and freshwater diatoms (17 - 24%) becoming relevant in the sediment trap assemblage. Nevertheless, during upwelling productive seasons, the diatoms exported out from surface layer reflected water column diatom assemblage. They were principally represented by *Chaetoceros* spp. (mean $46 \pm 25\%$) and *Leptocylindrus* spp. (mean $20 \pm 22\%$) resting spores, demonstrating that both groups are a good sedimentary imprint during highly productive periods. Moreover, our data showed that the sink of *Chaetoceros* spp. resting spores dominated under persistent upwelling winds, high irradiance levels and cold and nutrient-rich waters. Otherwise, *Leptocylindrus* spp. spore fluxes were favoured when northerly winds relax, and surface waters warming promotes water column stratification. Further, this finding will provide a proxy of persistent vs. intermittent upwelling conditions, which is of particular relevance in palaeoceanography.

25 **Keywords:** diatoms; coastal upwelling; organic carbon; biogenic silica; sediment trap; NW Iberian;



1 Introduction

The ocean plays a critical role in the global carbon cycle as a vast reservoir that takes up a substantial portion of the anthropogenically-released carbon from the atmosphere (LeQuéré et al., 2009). A key aspect to understand the ocean carbon cycle includes the fixation of atmospheric CO₂ by diatoms (Falkowski et al., 1998; Smetacek, 1999; Boyd and Trull, 2007).

5 These microorganisms, which are the most important global producers respond to environmental characteristics in the upper water column. In addition, they play a key role as sinkers of particulate organic carbon and biogenic silica from the surface productive layer to the sediment record (Sancetta, 1989; Romero and Armand, 2010; Tréguer and De La Rocha, 2013). All these points underpin the importance and the effectiveness of diatom species as productivity indicators in Earth's climate system studies. Nevertheless, primary production reconstructions suffer from the uncertainty about how diatoms respond to particular environmental conditions, and how particular diatom species transfer primary production signal via exported and buried particles. Therefore, to better understand and quantify past productivity conditions from sediment cores, regional calibrations are required.

15 Coastal upwelling systems as sites of major primary production, with a marked seasonality are thus ideal for these types of studies (Walsh, 1991; Falkowski et al., 1998; Capone and Hutchins, 2013). Consequently, many works have been focused on the study of diatom fluxes in highly productive coastal regions with the aim to better understand the diatom signal at longer time scales (Sancetta, 1995; Lange et al., 1998; Romero et al., 2002; Abrantes et al., 2002; Venrick et al., 2003; Onodera et al., 2005).

20 In the NW Iberian continental margin, seasonal upwelling favouring winds generate high primary production rates through modulation of the microplankton community structure (Figueiras and Pazos, 1991; Nogueira and Figueiras, 2005; Espinoza-González et al., 2012). Although there are no previous studies using long-term sediment traps for the NW Iberian margin, several works have assessed the diatom species ecology - environmental conditions relationship by comparing the recent sediment record to the hydrographic conditions (Abrantes, 1988; Bao et al., 1997; Abrantes and Moita, 1999; Gil et al., 2007; Bernárdez et al., 2008; Abrantes et al., 2011). Those authors concluded that the spatial distribution of the sedimentary diatom abundance and assemblages' composition reflects the hydrographic upwelling patterns and primary production trends, with *Chaetoceros* resting spores appearing as a good tracer of the upwelling regime.

25 The aim of this study is to evaluate the use of marine diatoms as a paleoproductivity proxy for the NW Iberian coastal upwelling system. This work presents the first diatom assemblage analysis that combines samples from the water column, sediment trap and surface sediment samples to understand the mechanisms regulating the export of specific diatoms species from the photic zone into the seafloor sediments.

30 2 Regional setting

Our study site (RAIA station) is located in the NW Iberian continental shelf off Cape Silleiro (42° 05' N; 8° 56' W at 75 m water depth, Fig. 1). During spring – summer, the NW Iberian coast is characterized by prevailing northerly winds, that



favour upwelling of cold and nutrients rich subsurface Eastern North Atlantic Central Water (ENACW) on the shelf and into the Rías, resulting in a primary production increase in the area (Fraga, 1981; Fiuza, 1984; Tenore et al., 1995; Figueiras et al., 2002). In contrast, south-westerly winds favour coastal downwelling during autumn-winter. From October to January the region is generally affected by the northward advection of warm, saline and nutrient-poor southerly waters by the Iberian Poleward Current (IPC) (Haynes and Barton, 1990, Relvas et al., 2007). Later on, usually between February–March, a decrease of temperature associated with winter cooling leads to a well homogenized mixed layer of cold and nutrient rich waters (Álvarez–Salgado et al., 2003; Castro et al., 2006). In addition, during downwelling seasons, the occurrence of south-westerly winds in this high-energy dynamic margin can generate moderate to extreme storms with wave heights > 6 m, which have been simulated to produce high sediment remobilization (> 50 %) (Vitorino et al., 2002; Jouanneau et al., 2002; Oberle et al., 2014). During these hydrodynamic periods, this site is also highly influenced by the Minho and Douro Rivers discharge, which provide important sources of terrestrial sediments to the inner shelf (Dias et al., 2002).

3 Material and methods

3.1 External forcing

Irradiance data was obtained from Cies meteorological station (IR; 42° 13'N, 8° 54'W; 25 m height) supported by Galician government and accessed at MeteoGalicia website (www2.meteogalicia.es) (Fig. 1).

Daily Ekman transport ($-Q_x$), an estimate of the volume of upwelled water per kilometre of coast was calculated according to Bakun's (1973) method:

$$-Q_x = -((\rho_a CD |V|) / (f \rho_{sw})) V_y$$

where ρ_a is the density of the air (1.22 kg m^{-3}) at 15°C , CD is an empirical dimensionless drag coefficient ($1.4 \cdot 10^{-3}$), f is the Coriolis parameter ($9.76 \cdot 10^{-5}$) at 42°N , ρ_{sw} is the seawater density (1025 kg m^{-3}) and $|V|$ and V_y are the average daily module and northerly component of the geostrophic winds centred at 42°N , 10°W , respectively. Positive values show the predominance of northerly winds that induces upwelling on the shelf and negative values indicate the presence of downwelling. Minho and Douro River discharges were obtained from https://github.com/PabloOtero/uptodate_rivers (Otero et al., 2010). Wave data were based on WANA hindcast reanalysis of 3027034 (WANA_S: off Silleiro: $42^\circ 15' \text{N}$; 9°W) and 1044067 (WANA_G: off A Guardia: $41^\circ 45' \text{N}$; 9°W) points, and supplied by Puertos del Estado (Fig. 1).

3.2 Water column

RAIA station (75 m water depth) was visited monthly on board “R/V *Mytilus*” from March 2009 to June 2012 except during the period December 2009–June 2010. Characterization of the water column was conducted by i) CTD-SBE25 profiling and



ii) collection of discrete water column samples using a rosette sampler with 10-LPVC Niskin bottles for inorganic nutrients, chlorophyll *a* (Chl *a*) analysis and diatoms counting and species identification.

Water column stability (0-35 m) was analysed by using Brunt Väisälä frequency parameter, $N^2 = [g / z] \ln (p_z/p_0)$ where *g* is the local acceleration of gravity, *z* is the water depth and *p_z* and *p₀* the bottom and surface density, respectively.

5 Nutrients concentration was determined by segmented flow analysis with Alpkem autoanalysers (Hansen and Grasshoff, 1983). The analytical errors were $\pm 0.05 \mu\text{mol kg}^{-1}$ for nitrate and silicate and $\pm 0.01 \mu\text{mol kg}^{-1}$ for phosphate. Final Chl *a* concentrations were determined by pigment extract fluorescence using a Turner Designs fluorometer calibrated with pure Chl *a* (Sigma) (please see details in Zúñiga et al., 2016).

For diatoms counting and identification a seawater volume of 100 ml collected at 5 m water depth was preserved with
10 Lugol's iodine until microscopic observation. Depending on the water column Chl *a* concentration volumes between 10 to 50 mL were deposited in composite sedimentation chambers and observed through an inverted microscope. The microorganisms were counted and identified to the species level, whenever possible, using the Utermöhl sedimentation method (Utermöhl, 1931, 1958). For this study only water column diatom species that appeared in more than one sample with a percentage higher than 2 % of the total abundance were considered for further analysis primary production.

15 3.3 Sediment trap

RAIA station was monitored with an automated cylindrical-conical Technicap PPS 4/3 sediment trap (height/diameter ratio of 1.7 and a collecting area of 0.05 m^2) from March 2009 to June 2012 (Zúñiga et al., 2016). The trap was deployed at 35 m
20 water depth over sampling intervals between 4-12 days. Examination of CTD pressure data mounted 2 m below the sediment trap showed that the mooring line tilting was less than 5° during 70 % of the time it was deployed. Only in exceptional cases highly hydrodynamic events lead to velocities higher than 25 cm s^{-1} and mooring tilts between $15\text{-}20^\circ$. Therefore, we can assume that the trap was not affected by hydrodynamical biases. Sampling strategy and samples processing details are explained at length in Zúñiga et al. (2016).

Total mass flux was gravimetrically determined. Biogenic silica content was analysed following Mortlock and Froelich, (1989). The samples were treated with $2\text{M Na}_2\text{CO}_3$ for 5 h at 85°C to extract the silica and then measured as dissolved silica
25 by colorimetric reaction. Biogenic opal was converted from Si concentration after multiplying it by a factor of 2.4.

Sample preparation for diatom abundance and assemblage assessment was adapted from Abrantes et al. (2005). Depending on the recovered material 1/5 or 2/5 splits of the original samples were used, after rinsing HgCl_2 by repeated settling in distilled water. Subsequently, organic matter and carbonates were removed by the addition of H_2O_2 (30 %) and HCl (10 %), respectively. Permanent slides were prepared using the evaporation-tray method of Battarbee, (1973) and mounted with
30 Norland optical adhesive (NOA61). Diatoms counting and species identification was performed at 1000 X (10 x eyepieces and 100 x objectives), using a Nikon Eclipse E100 microscope equipped with Differential Interference Contrast (DIC). 100 randomly selected fields of view were counted in 3 replicate slides (Abrantes et al., 2005). Diatom flux was calculated as



$$F = ((N)(A/a) (V)(S)(X))/D$$

where the flux F is expressed as number of valves $m^{-2} d^{-1}$, N is the number of valves counted in 100 randomly selected fields of view, (a) represents the counted fraction of the total tray area (A), V is the dilution volume, S is the split fraction, X is the conversion factor from the collecting area to $1 m^2$, and D is the sampling interval in days for each sample.

- 5 Relative abundance of diatom taxa was determined following the counting procedures from Schrader and Gersonde, (1978) and Abrantes, (1988). For each sample, ca. 300 individuals were identified to the lowest taxonomic possible level, and raw counts were converted to percentage abundance. In samples containing low diatom abundances, the number of individuals identified was 100 – 200 (Fatela and Taborda, 2002). For this study only sediment trap diatom species that appeared in more than one sample with a percentage higher than 2% of the total abundance were considered for further analysis.

10 3.4 Surface sediments

Surface sediments (0 - 1 cm depth interval) were recovered from GeoB 11002-1 (42° 10' N, 8° 58' W; 111 m) and GeoB 11003-2 (42° 10' N, 9° 1' W; 129 m) stations located near the RAIA position (Fig. 1). Samples were collected in August 2006, using a giant box corer during the GALIOMAR expedition (P342) on board of the R/V *Poseidon*. Sample cleaning and slides preparation of the samples was carried out following the methodology of Abrantes et al. (2005). Counting and
 15 identification procedures were the same as for sediment traps samples.

3.5 Statistical data analysis

Relationships between environmental variables and diatoms species from the sediment trap record were evaluated with Pearson correlation coefficients (Table 1 and 2).

- The relationships between the main groups of diatoms (freshwater diatoms, benthic diatoms, *Chaetoceros* resting spores, *Leptocylindrus* resting spores and *Paralia sulcata*) and the environmental variables were analysed using the ordination technique Canonical Correspondence Analysis (vegan package, R-project (ter Braak, 1986; Oksanen et al., 2015). Environmental data used for this analysis resulted from water column data interpolation by considering sediment trap sample recovering intervals. Resulting data were subsequently integrated to 35 m where the sediment trap was moored. The multicollinearity of environmental variables was previously tested by Pearson correlations (Dormann et al., 2013) and
 25 checked after modelling using variance inflation factors (VIFs) applied to the CCA. Nine environmental variables were thus initially included in the ordination: irradiance, temperature, Brunt Väisälä frequency parameter (N^2), Chl a , NO_3 , $Si(OH)_4$, upwelling index (UI), Minho River flow, A Guarda wave height (Hs). Significant environmental variables were identified via a stepwise procedure, using permutation tests (999 permutations). After the selection of the significant variables, the model was tested a second time through a Monte Carlo global permutation test (999 permutations) to assess the significance
 30 of ordination axes.



The results of CCA were presented as ordination bi-plot diagram containing the explanatory variables plotted as arrows along with points for samples (dates) and species (main groups of diatoms). Using these diagrams, we were able to identify the relationships between species, between samples, and relationships of samples and species to environmental variables.

4 Results

5 4.1 Environmental conditions and water column characteristics

From October to April-May, the NW Iberian margin was generally characterized by the prevalence of low irradiance levels and south-westerly winds as shown by the negative $-Q_x$ values (Fig. 2a and 2b). This downwelling season was also accompanied of strong SW storms promoting wave heights frequently higher than 4 m and intense Minho and Douro River discharges (Fig. 2c and 2d). Hydrographically, in a first phase we can distinguish the presence of the IPC (October-January) characterized by anomalously warm water (15-17 °C) with relatively low nutrient and Chl a ($< 4 \text{ mg m}^{-3}$) content (Fig. 3). Later on, we differentiate the mixing period with temperatures around 14 °C and higher nutrient levels due to winter cooling. Furthermore, river runoff promoted water column stability through the formation of low salinity water lens at sea surface with significant loads of silicate-rich particulate matter (Fig. 2c, 3a, 3b and Table 1). During downwelling periods, diatom abundances were low ($\sim 14 \text{ cel mL}^{-1}$) (Fig. 3c). Small centric cells accounted for the largest shares (37–84 %) and only exceptionally *Navicula* spp. and *Paralia sulcata* become relevant (Fig. 4b and 4d). From May to October, when irradiance levels remained high, a series of upwelling relaxation events promoted the upwelling of cold ($< 14^\circ\text{C}$) and nutrient rich ENACW on the continental shelf, leading to the development of Chl *a* maxima (Fig. 3). During the highly productive upwelling seasons, diatom abundances achieved maximum levels (up to 7629 cel mL^{-1}) (Fig. 3c), and the predominant genera were *Chaetoceros* and *Leptocylindrus* spp. (Fig. 4f). Other species frequently associated with upwelling favourable conditions (e.g. *Asterionellopsis glacialis*, *Detonula pumila* or *Guinardia delicatula*), appeared in the upper water column, sporadically and with lower abundances (Fig. 4g and 4h).

4.2 Sinking particulate material time series

Time series of the siliceous organism fluxes calculated from microscopic counting matched biogenic silica fluxes registered by the trap, which contribution to the total material ranged from 2 % to 10 % (Fig. 5a, 5b and 5c). The contribution of diatoms to total siliceous microorganisms was high during all study years (Fig. 5c and 5e). Only during the 2012 upwelling season, silicoflagellates become relevant, achieving more than 7 % of the total siliceous organisms (Fig. 5d). Maximum total diatom fluxes (up to up to $22.6 \cdot 10^6 \# \text{ m}^{-2} \text{ d}^{-1}$) were registered under downwelling conditions when benthic and freshwater



diatoms fluxes became relevant, with contributions to the total diatom fluxes up to 24 % and 17 %, respectively (Fig. 5e and 6).

Regarding the fluxes of marine diatom assemblage, during downwelling periods, small centric diatoms and additionally *Paralia sulcata* significantly contributed to the total marine diatom fluxes with percentages achieving maximum values of 11 % and 54 %, respectively (Fig. 7a, 7b, 7c, 7d). On the contrary, under upwelling favourable conditions, the marine diatom assemblage found in the trap were mainly composed by *Chaetoceros* and *Leptocylindrus* spp. resting spores with contributions to total marine diatom fluxes fluctuating around mean seasonal values of 46 % and 20 %, respectively (Fig. 7a, 7b and Table 3).

4.3. Surface sediment samples

10 Diatom abundances in GeoB 11002-1 top sediment sample was significantly higher than in the offshore GeoB 11003-2 station with values of 142×10^4 # valves gr^{-1} and 65×10^4 # valves gr^{-1} respectively (Table 3). Diatom assemblages were similar at both sampling sites, with predominance of *Chaetoceros* spp. (33-39%) and *Leptocylindrus* spp. (37-39 %) resting spores and *Paralia sulcata* (10-17 %) (Table 3). Otherwise, benthic and freshwater diatoms have a significantly lower contribution (< 4 % and 1 %, respectively) at both stations.

15 4.4 Relationships between sediment trap main diatom groups and environmental variables

Canonical correspondence analysis (CCA) stepwise procedure identified five significant variables (Minho River flow (Minho river), temperature (Temp), Chlorophyll *a* (Chl *a*), NO_3 and Si(OH)_4) for the abundance of the main diatom groups (p -value < 0.05) (Fig. 8). The first two canonical axes explained 48.7 % and 40.4 %, i.e. 89 % of the modelled inertia and consequently only those two axes were considered. The CCA model with the five variables explained 46% of the total inertia. The first canonical axis showed a positive gradient with Temp and Chl *a* opposite to Minho River discharge. Freshwater (FW) diatoms, benthic diatoms and *Paralia sulcata* (Parsul) were negatively positioned in the first canonical axis, indicating thus a positive relationship with Minho River, and negative with temperature and Chl *a*. The second canonical axis showed a negative gradient with NO_3 and Si(OH)_4 and a negative relationship of these variables to *Chaetoceros* resting spores (ChaeRS). Conversely, *Leptocylindrus* resting spores (LepRS) were positively related with NO_3 and Si(OH)_4 . The temporal distribution of the sediment trap samples showed that FW diatoms, benthic diatoms and Parsul occurred mainly during downwelling months while ChaeRS and LepRS were associated to upwelling periods (Fig. 8). Besides, this figure also discerns a location of LepRS towards the late summer and IPC periods.



5 Discussion

The siliceous microorganism fluxes, mostly represented by diatoms in both vegetative and resting spore stages, were strongly linked to biogenic silica fluxes and presented abrupt changes along the entire time series (Fig. 5). The observed temporal variability was determined by the regional hydrodynamic conditions at the NW Iberian inner continental margin, as explained in detail by Zúñiga et al. (2016). These authors described how maximum particle fluxes occurring during downwelling periods were associated with resuspension processes mainly driven by wave action. This finding explains the a priori contradictory observation of maximum diatom fluxes during downwelling periods, when irradiance conditions were unfavourable and Chl *a* showed its minimum levels (Fig. 2, 3c and 5e). Conversely, during highly productive upwelling periods, even though biogenic silica fluxes were relatively low, diatoms contribution (including resting spores stage) achieved maximum percentages (Fig. 5e and 5f). Therefore, our results confirm the major influence of the hydrodynamic conditions and seasonal productivity over the diatoms export to the surface sediment in this coastal upwelling system.

5.1. Sediment trap diatom assemblage as a tracer of allochthonous sources in sinking material

Maximum fluxes of benthic diatoms, whose natural habitat is the sediment interface, run parallel with higher wave heights during highly hydrodynamic downwelling periods (Fig. 2c and 6a), confirming that strong storms resuspended surface sediments at the inner Iberian continental shelf (Dias et al., 2002; Vitorino et al., 2002. Jounneau et al., 2002, Oberle et al., 2014). Furthermore, stormy conditions were accompanied by intense Minho and Douro River discharges, resulting in lower salinity water lens at the sea surface, which had a significant effect over the water column thermohaline structure (Fig. 2d and 3a). The significant increase in freshwater diatoms associated to river runoff confirms how continental inputs constituted an additional source of terrestrial material to the inner continental shelf (Fig. 2c and 6c). Indeed, canonical analysis of sediment trap samples revealed a high correlation between benthic and freshwater diatoms, corroborating the co-occurrence of both resuspension processes and river discharges during downwelling periods (Fig. 8 and Table 2).

One additional evidence of resuspension resulted from the analysis of marine diatom assemblage collected in the sediment trap. *Paralia sulcata* was sporadically found in the water column diatom assemblage during the 2009-2012 studied years (Fig. 4c and Table 3). This meroplanktonic and shadow species, it is by contrast, common in the sediments and highly contributed to the diatom fluxes during downwelling phases (Fig. 7c and Table 3). This observation can only be explained by the fact that *Paralia sulcata* is a robust and highly silicified species, relatively more resistant to dissolution processes, that gets enriched in the sediments. Consequently, and as pointed out by previously published sediment trap data from the adjacent Ría de Vigo (Bernárdez et al., 2010; Zúñiga et al., 2011), our data confirms it as a species that can be easily resuspended from the sediments under highly hydrodynamic conditions. This is, in fact, also exposed by the positive relationship found between *Paralia sulcata* and benthic diatoms in the trap samples (Fig. 8 and Table 2). Also interesting is the positive correlation between freshwater and benthic diatoms to *Thalassiosira eccentrica* (Table 2), a species which is



known to occur in areas where nutrient input is continuous throughout the year, such as in areas influenced by river discharge (Moita, 1993, Abrantes and Moita, 1999).

5.2 Seasonal succession of diatom species during upwelling seasons: the imprint over the fossil diatom assemblage

During the studied period, the living diatom community was strongly linked to the seasonality revealed by environmental variables, with the highest abundances always recorded during upwelling favourable periods, when irradiance and water column characteristics promote favourable conditions for diatom growing (Fig. 2a and 3).

A detailed analysis of the marine diatom assemblage during upwelling productive seasons revealed that most living species linked to upwelling favourable conditions were not found (e.g. *Asterionellopsis glacialis*, *Detonula pumila*, *Guinardia delicatula* and *Skeletonema costatum*) or appeared with a significant lower contribution (e.g. *Nitzschia* spp., *Pseudonitzschia* spp. and small centric) in the diatom assemblages on both the sediment trap and the surface sediment samples (Table 3). This observation points to selective dissolution processes acted over thin-walled, less silicified diatoms. As a result, the robust and heavily silicified frustules, not only have a ballast effect that promotes a faster arrival to the sediments, as have a higher preservation potential in the seafloor sediments. Indeed, diatoms assemblages in both sediment trap and surface sediment samples were mainly represented by the highly resistant *Chaetoceros* and *Leptocylindrus* spp. resting spores (Table 3). This fact confirms these diatom genera as a good sedimentary imprint of highly productive upwelling conditions. Moreover, the sink of *Chaetoceros* and *Leptocylindrus* spp. resting spores, occurring in close correlation with the dominance of both diatom groups in the water column assemblage during the upwelling periods (Table 3), brings new important information to previous works carried out along the Iberian margin which have only considered *Chaetoceros* spp. resting spores group as tracer of the coastal upwelling regime (Abrantes, 1988; Bao et al., 1997; Abrantes and Moita, 1999). Certainly, canonical analysis performed for the sediment trap data, with *Chaetoceros* and *Leptocylindrus* spp. spores reflecting upwelling favourable conditions (positively positioned in CCA1), also showed the two genera differently placed with respect to significant environmental variables (Fig. 8). Overall, the sink of *Chaetoceros* spp. resting spores out from the photic zone was mostly associated to spring-summer periods (Fig. 8), revealing the onset of the upwelling seasons when irradiance conditions are favourable and persistent northerly winds lead to the upwelling of nutrient-rich subsurface ENACW waters on the shelf (Fig. 3, 4e and 4f) (Figueiras and Rios, 1993; Nogueira and Figueiras, 2005). Otherwise, *Leptocylindrus* spp. resting spores fluxes at the base of the photic layer were significantly associated to late-summer autumn (Fig. 8), marking highly productive upwelling periods (as shown by Chl *a* levels) when the relaxation of winds promotes water column stratification due to surface warming, and nutrients associated to upwelling (nitrates and phosphates) become depleted (Fig. 3, 4e and 4f) (Escaravage et al., 1999; Casas et al., 1999; Nogueira and Figueiras, 2005). In summary, even though we do not dispose of a quantitative estimate of water column/sediment record preservation efficiencies due to strong resuspension processes remobilized bottom sediments at the inner NW Iberian continental shelf, our results expose an important role of *Chaetoceros* and *Leptocylindrus* spp. resting spores during the highly productive



upwelling intervals. Indeed, our data comprise important implications for paleoceanographic and paleoclimatic studies, since a careful evaluation of the *Chaetoceros* and *Leptocylindrus* spp. spores contribution to the total marine diatom assemblage present in the sediment records should allow the identification of persistent vs intermittent upwelling favourable winds, with *Leptocylindrus* spp. spores being more abundant in an intermittent upwelling mode.

5 Acknowledgements

The authors gratefully thank the crew of “R/V *Mytilus*” for their valuable help during the cruises. The authors also want to specially recognize specific lab work made from different members of both the Oceanography group from the Instituto de Investigaciones Marinas de Vigo (CSIC) and the Divisão de Geologia e Georecursos Marinhos from Instituto Português do Mar e da Atmosfera (IPMA). Special thanks to M. Zúñiga for his help in the writing process. This study was sponsored by CAIBEX (CTM2007-66408-C02-01/MAR) and REIMAGE (CTM2011–30155–C03–03) projects funded by the Spanish Government, EXCAPA project (10MDS402013PR) supported by Xunta de Galicia, the EU FEDER funded projects RAIA (INTERREG 2009/2011-0313/RAIA/E) and RAIA.co (INTERREG 2011/2013-052/RAIA.co/1E) and the CALIBERIA project (PTDC/MAR/102045/2008) financed by Fundação para a Ciência e a Tecnologia (FCT-Portugal). D.Z. and E.S. were funded by a postdoctoral fellowship (Plan I2C) from Xunta de Galicia (Spain) and (SFRH/BPD/111433/2015) from FCT, respectively. C.S. was funded by a doctoral grant from FCT (Portugal) (SFRH/BD/88439/2012).

References

- Abrantes, F., 1988. Diatoms assemblages as upwelling indicators in surface sediments in Portugal. *Mar. Geol.* 85, 15-39.
- Abrantes, F., Moita, M.T., 1999. Water column and recent sediment data on diatoms and coccolithophorids, off Portugal, confirm sediment record of upwelling events. *Oceanol. Acta*, 22(1), 67-84.
- Abrantes, F., Meggers, H., Nave, S., Bollman, J., Palma, S., Sprengel, C., Henderiks, J., Spies, A., Salgueiro, E., Moita, T., Neuer, S., 2002. Fluxes of micro-organisms along a productivity gradient in the Canary Islands region (29°N): implications for paleoreconstructions. *Deep Sea Res. II*, 49, 3599-3629.
- Abrantes, F., Gil, I., Lopes, C., Castro, M., 2005. Quantitative diatom analyses: a faster cleaning procedure. *Deep Sea Res. II* 52, 189-198.
- Abrantes, F., Rodrigues, T., Montanari, B., Santos, C., Witt, L., Lopes, C., Voelker, A.H.L., 2011. Climate of the last millennium at the southern pole of the North Atlantic Oscillation: an inner-shelf sediment record of flooding and upwelling. *Clim. Res.* 48, 261-280.



- Álvarez-Salgado, X.A., Figueiras, F.G., Pérez, F.F., Groom, S., Nogueira, E., Borges, A.V., Chou, L., Castro, C.G., Moncoiffé, G., Ríos, A.F., Miller, A.E.J., Frankignoulle, M., Savidge, G., Wollast, R., 2003. The Portugal coastal counter current off NW Spain: new insights on its biogeochemical variability. *Prog. Oceanogr.* 56, 281-321.
- Bakun, A., 1973. Coastal upwelling Indices, West Coast of North America, 1946-71. US Department of Commerce, National Oceanic and Atmospheric Administration, National Marine Fisheries Service, Seattle, WA.
- Bao, R., Varela, M., Prego, R., 1997. Mesoscale distribution patterns of diatoms in surface sediments as tracers of coastal upwelling of the Galician shelf (NW Iberian Peninsula). *Mar. Geol.* 144, 117-130.
- Battarbee, R. W. 1973. A new method for estimating absolute microfossil numbers with special reference to diatoms. *Limnol. Oceanogr.* 18, 647-653.
- 10 Bernárdez, P., Prego, R., Varela, M., Francés, G., 2008. Diatom thanatocoenosis in a middle Galician Ría: Spatial patterns and their relationship to the seasonal diatom cycle in the water column and hydrographic conditions. *Cont. Shelf Res.* 28, 2496-2508.
- Bernárdez, P., Varela, M., Pazos, Y., Prego, R., Francés, G., 2010. Biocenosis and thanatocoenosis of diatoms in a western Galician ría. *J. Plank. Res.* 32 (6), 857-883.
- 15 Boyd, P.W., and Trull, T.W., 2007. Understanding the export of biogenic particles in oceanic waters: Is there consensus?. *Progr. Oceanogr.* 72, 276-312.
- Capone, D.G., Hutchins, D.A., 2013. Microbial biogeochemistry of coastal upwelling regimes in a changing ocean. *Nature*, 6, 711-717, doi: 10.1038/ngeo1916.
- Casas, B, Varela, M., Bode, A., 1999. Seasonal succession of phytoplakton species on the coast of A Coruña (Galicia, Northwest Spain). *Boletín del Instituto Español de Oceanografía*, 15, 413-429.
- 20 Castro, C.G., Nieto-Cid, M., Álvarez-Salgado, X.A., Pérez, F.F., 2006. Local remineralization patterns in the mesopelagic zone of the Eastern North Atlantic, off the NW Iberian Peninsula. *Deep Sea Res. I*, 53, 1925-1940.
- Dias, J.M.A., González, R., García, C., Díaz-del-Río, V., 2002. Sediment distribution patterns on the Galicia–Minho continental shelf. *Prog. Oceanogr.* 52 (2–4), 215–231.
- 25 Dormann, C.F., Elith, J., Bacher, S., Buchmann, C., Carl, G., Carré, G. et al. 2013. Collinearity: a review of methods to deal with it and a simulation study evaluating their performance. *Ecography* 36: 27-46.
- Escaravage, V., Prins, T.C., Nijdam, C., Smaal, A.C., Peeters, J.C.H., 1999. Response of phytoplankton communities to nitrogen input reduction in mesocosm experiments. *Mar. Ecol. Prog. Series* 179, 187-199.
- Espinoza-González, O., Figueiras, F.G., Crespo, B., Teixeira, I.G., Castro, C.G., 2012. Autotrophic and heterotrophic microbial plankton biomass in the NW Iberian upwelling: seasonal assessment of metabolic balance. *Aquat. Microb. Ecol.* 30, 67, 77-89.
- Falkowski, P.G., Barber, R.T., Smetacek, V., 1998. Biogeochemical controls and feedbacks on ocean primary production. *Science*, 281, 200.



- Fatela, F., Taborda, R., 2002. Confidence limits of species proportions in microfossil assemblages. *Mar. Micropaleontol.* 45, 169-174.
- Figueiras, F.G., Pazos, Y., 1991. Microplankton assemblages in three Rías Baixas (Vigo, Arosa and Muros, Spain) with a subsurface chlorophyll maximum: their relationships to hydrography. *Mar. Ecol. Prog. Ser.* 76, 219-233.
- 5 Figueiras, F.G., Rios, A.F., 1993. Phytoplankton succession, red tides and the hydrographic regime in the Rias Bajas of Galicia. In: *Toxic Phytoplankton Blooms in the Sea*. T.J., Smayda and Y. Shimizu, Ed. Elsevier Science Publishers B.V., pp, 239-244.
- Figueiras, F.G., Labarta, U., Fernández Reiriz, M.J., 2002. Coastal upwelling, primary production and mussel growth in the Rías Baixas of Galicia. *Hydrobiologia*, 484, 121-131.
- 10 Fiuza, A.F.G., 1984. Hidrologia e dinâmica das águas costeiras de Portugal. Ph.D. Thesis, Faculdade de Ciências, Univ. Lisboa, Portugal.
- Fraga, F., 1981. Upwelling off the Galician coast, north west of Spain. In: Richards, F. (Ed.), *Coastal Upwelling*. American Geophysical Union, Washington, pp. 176-182.
- Gil, I., Abrantes, F., Hebbeln, D., 2007. Diatoms as upwelling and river discharge indicators along the Portuguese margin: instrumental data linked to proxy information. *The Holocene*, 17 (8), 1245-1252.
- 15 Hansen, H.P. and Grasshoff, K., 1983. Automated chemical analysis. In: Grasshoff, K., Ehrhardt, M., and Kremling, K. (Eds). *Methods of seawater analysis*. Verlag Chemie, Weinheim, p.p. 347-395.
- Haynes, R., Barton, E.D., 1990. A poleward flow along the Atlantic coast of the Iberian Peninsula. *J. Geophys. Res.* 95, 11425-11442.
- 20 Jouanneau, J.M., Weber, O., Drago, T., Rodrigues, A., Oliveira, A., Dias, J.M.A. et al., 2002. Recent sedimentation and sedimentary budgets on the western Iberian shelf. *Prog. Ocenogr.* 52, 261-275.
- Lange, C.B., Romero, O.E., Wefel, G., Gabric, A.J., 1998. Offshore influence of coastal upwelling off Mauritania, NW Africa, as recorded by diatoms in sediment traps at 2195 m water depth. *Deep Sea Res. I*, 45, 985-1013.
- LeQuéré, C., Raupach, M., Canadell, J.G., Marland, G. et al., 2009. Trends in the sources and sinks of carbon dioxide. *Nature Geoscience*, doi: 10.1038/ngeo689.
- 25 Moita, T., 1993. Spatial variability of phytoplankton communities in the upwelling region off Portugal, *Proceedings of the International Council for the Exploration of the Sea*, L64, 1-20.
- Mortlock, R.A., Froelich, P.N., 1989. A simple method for the rapid determinations of biogenic opal in pelagic marine sediments. *Deep Sea Res.* 36 (9), 1415-1426.
- 30 Nogueira, E., Figueiras, F.G., 2005. The microplankton succession in the Ría de Vigo revisited: species assemblages and the role of weather-induced, hydrodynamic variability. *J. Mar. Sys.* 54, 139-155.
- Oberle, F.K.L., Storlazzi, C.D., Hanebuth, T.J.J., 2014. Wave-driven sediment mobilization on a storm-controlled margin. *J. Mar. Sys.* 139, 362-372.



- Oksanen J., Blanchet F. G., Kindt R., Legendre P., Minchin P. R., O'Hara R. B., et al. (2015). Vegan: Community ecology. Available online at: <http://CRAN.R-project.org/package=vegan>.
- Onodera, J., Takahashi, K., Honda, M.C., 2005. Pelagic and coastal diatom fluxes and the environmental changes in the northwestern North Pacific during December 1997-May 2000. *Deep Sea Res. II*, 52, 2218-2239.
- 5 Otero, P., Ruiz-Villarreal, M., Peliz, A., Cabanas, J.M., 2010. Climatology and reconstruction of runoff time series in northwest Iberia: influence in the shelf buoyancy budget off Ría de Vigo. *Sci. Mar.* 74 (2), 247-266.
- Relvas, P., Barton, E.D., Dubert, J., Oliveira, P.B., Peliz, A., da Silva, J.C.B., Santos, A.M.P., 2007. Physical oceanography of the western Iberia ecosystem: Latest views and challenges. *Prog. Oceanogr.* 47, 149-173.
- Romero, O.E., Lange, C.B., Wefer, G., 2002. Interannual variability (1988-1991) of siliceous phytoplankton fluxes off
10 northwest Africa. *J. Plankton Res.* 24 (10), 1035-1046.
- Romero, O.E., Armand, L.K., 2010. Marine diatoms as indicators of modern changes in oceanographic conditions. In: *The Diatoms: Applications for the Environmental and Earth Sciences*, 2nd Edition, eds. John P. Smol and Eugene F. Stoermer. Published by Cambridge University Press. © Cambridge University Press, pp. 373-400.
- Sancetta, C., 1989. Processes controlling the accumulation of diatoms in sediments: a model derived from the british
15 columbian fjords. *Paleoceanography*, 4 (3), 235-251.
- Sancetta, C., 1995. Diatoms in the Gulf of California: seasonal flux patterns and the sediment record for the last 15 000 years. *Paleoceanography*, 10(1), 67-84.
- Schrader, H. J., and Gersonde, R., 1978. Diatoms and silicoflagellates. *Utrecht Micropaleontol. Bull.*, 17:129-176.
- Smetacek, V., 1999. Diatoms and the Ocean Carbon Cycle. *Protist*, 150, 25-32.
- 20 Tenore, K. R., Alonso-Noval, M., Álvarez -Ossorio, M., Atkinson, L.P., Cabanas, J. M., et al., 1995. Fisheries and oceanography off Galicia, NW Spain: Mesoscale spatial and temporal changes in physical processes and resultant patterns of biological productivity. *J. Geophys. Res.* 100(C6), 10943-10966.
- ter Braak, C. J. F. 1986. Canonical correspondence analysis: a new eigenvector technique for multivariate direct gradient analysis. *Ecology*, 67, 1167-1179.
- 25 Tréguer, P.J., De La Rocha, C.L., 2013. The world Ocean Silica Cycle. *Annu. Rev. Marine Sci.* 5, 477-501.
- Utermöhl, H., 1931. Neue Wege in der quantitativen Erfassung des Planktons (mit besonderer Berücksichtigung des Ultraplanktons). *Verh. int. Ver. theor. angew. Limnol.* 5: 567-596.
- Utermöhl, H., 1958. Zur Vervollkommnung der quantitativen Phytoplankton-Methodik. *Mitt. int. Ver. ther. angew. Limnol.* 9: 1-38.
- 30 Venrick, E.L., Reid, F.M., Lange, C.B., 2003. Siliceous phytoplankton in the Santa Barbara Channel: a seven-year comparison of species in a near-bottom sediment trap and in water samples from the euphotic layer. *CalCOFI Rep.*, Vol. 44.
- Vitorino, J., Oliveira, A., Jouanneau, J.M., Drago, T., 2002. Winter dynamics on the northern Portuguese shelf. Part 2: bottom boundary layers and sediment dispersal. *Progr. Oceanogr.* 52 (2-4), 155-170.



Walsh, J.J., 1991. Importance of continental margins in the marine biogeochemical cycling of carbon and nitrogen. *Nature*, 350, 53-55.

Zúñiga, D., Alonso-Perez, F., Castro, C.G., Arbones, B., Figueiras, F., 2011. Seasonal contribution of living phytoplankton carbon to vertical fluxes in a coastal upwelling system (Ría de Vigo, NW Spain). *Cont. Shelf Res.* 31, 414-424.

- 5 Zúñiga, D., Villaceros-Robineau, N., Salgueiro, E., Alonso-Pérez, F., Rosón, G., Abrantes, F., Castro, C.G., 2016. Particle fluxes in the NW Iberian coastal upwelling system: hydrodynamical and biological control. *Cont. Shelf Res.* doi: 10.1016/j.csr.2016.04.008.



Table 1. Environmental variables matrix Pearson correlations. Irrad: Irradiance; Temp: temperature; Sal: salinity; N^2 : Brunt Väisälä frequency parameter; Chl *a*: Chlorophyll *a*; SPM: suspended particulate matter; POC: particulate organic carbon; UI: Upwelling index; Minho: Minho River discharge; Waves: Significant wave height in A Guarda (WANA_G) station. Main relationships are highlighted with grey background.

5

	Irrad	Temp	Sal	N^2	Chl <i>a</i>	SPM	POC	NO_3	PO_4	$Si(OH)_4$	Oxygen	UI	Minho	Waves
Irrad	1.00	-0.394	0.487	-0.0827	0.528	-0.555	0.376	0.0167	0.0764	-0.642	0.148	0.487	-0.236	-0.357
Temp		1.00	-0.263	0.616	-0.196	0.332	0.184	-0.284	-0.195	0.351	-0.346	-0.456	0.0961	0.0557
Sal			1.00	-0.0509	0.228	-0.645	0.348	0.0839	0.263	-0.841	-0.137	0.518	-0.689	-0.27
N^2				1.00	-0.284	0.249	0.124	-0.266	0.0559	0.0825	-0.38	-0.266	-0.101	-0.0122
Chl <i>a</i>					1.00	-0.476	0.355	0.0608	-0.0003	-0.321	0.124	0.205	0.0433	-0.272
SPM						1.00	-0.104	0.153	0.0953	0.79	-0.223	-0.409	0.334	0.257
POC							1.00	0.24	0.341	-0.201	-0.39	0.0841	-0.246	-0.242
NO_3								1.00	0.871	0.287	-0.677	0.182	-0.106	-0.252
PO_4									1.00	0.137	-0.823	0.233	-0.274	-0.185
$Si(OH)_4$										1.00	-0.297	-0.466	0.523	0.240
Oxygen											1.00	0.0592	0.213	0.204
UI												1.00	-0.0394	-0.116
Minho													1.00	0.139
Waves														1.00



Table 2 Sediment trap diatom species matrix Pearson correlations that appear in more than one sample with percentages higher than 2% of the total abundance. FW: freshwater diatoms; ChaetoRS: *Chaetoceros* spp. resting spores; Cos. mar: *Coscinodiscus marginatus*; Cos. rad: *Coscinodiscus radiatus*; LeptoRS: *Leptocylindrus* spp. resting spores; Nav: *Navicula*; Nitzs.mar: *Nitzschia marina*; Par.sulc: *Paralia sulcata*; Pse.Pun: *Pseudo-nitzschia pungens*; Thal.ecc: *Thalassiosira eccentrica*; Thal.nitzs: *Thalassionema nitzschioides*. Main relationships are highlighted with grey background.

	FW	Benthic	ChaetoRS	Cos.mar	Cos.rad	LeptoRS	Nav.spp	Nitzs.mar	Par.sulc	Pse.pun	Thal.ecc	Thal.nitzs
FW	1.00	0.482	-0.0085	-0.312	0.161	0.226	-0.126	0.176	0.293	0.0318	0.382	-0.0879
Benthic		1.00	-0.38	0.267	0.51	-0.377	0.2	0.0623	0.671	0.159	0.428	0.0777
ChaetoRS			1.00	-0.315	-0.388	-0.0163	-0.147	-0.389	-0.493	-0.318	-0.337	-0.214
Cos.mar				1.00	0.416	-0.137	0.517	-0.138	0.201	0.15	0.182	0.253
Cos.rad					1.00	0.283	0.267	0.0427	0.487	0.0773	0.261	0.202
LeptoRS						1.00	-0.224	-0.107	-0.495	-0.185	-0.0972	-0.173
Nav.spp							1.00	-0.0424	0.196	0.18	0.074	0.174
Nitzs.mar								1.00	0.173	0.547	0.338	0.079
Par.sulc									1.00	0.113	0.288	0.0748
Pse.pun										1.00	0.412	0.561
Thal.ecc											1.00	0.451
Thal.nitzs.												1.00



Table 3. Total abundance and relative contributions of the marine diatom assemblage preserved in the water column, sediment trap and surface sediments samples, respectively. SD: Standard deviation. Nitzs: *Nitzschia*; Pseudo-nitzs: *Pseudo-nitzschia*; Thal. nitzs: *Thalassionema nitzschioides*; Nav: *Navicula*. Small centric in both sediment trap and surface sediment samples includes: *Coscinodiscus marginatus*, *Coscinodiscus radiatus*, *Thalassiosira eccentrica*; Chaet. and Lepto. spp: *Chaetoceros* and *Leptocylindrus* spp. cells and resting spores counted in the water column and sediment trap, respectively; Aster. glac: *Asterionellopsis glacialis*; Deton. pum: *Detonula pumila*, Guin. del: *Guinardia delicatula*, Skelet. cost: *Skeletonema costatum*. Most relevant species are highlighted in bold.

	Total	Nitzs. spp.	Pseudo-nitzs. spp.	Thal. nitzs.	Small centric	Nav. spp.	<i>Paralia sulcata</i>	Chaeto. spp	Lept. spp	Aster. glac.	Deton. pum.	Guin. del.	Skelet. cost.
WATER column													
Upwelling													
cel mL ⁻¹ (± SD)	717 (1869)	17 (50)	25 (30)	10 (17)	486 (1766)	1 (2)	0 (0)	72 (108)	126 (271)	3 (8)	17 (15)	11 (12)	1 (2)
% (± SD)		3(4)	16 (24)	0.1 (0.4)	20 (31)	0.1 (0.4)	0 (0)	27 (28)	26 (33)	1 (1)	3 (9)	2 (4)	2 (9)
Downwelling													
cel mL ⁻¹ (± SD)	34 (49)	2 (2)	12 (21)	1 (1)	10 (18)	0 (0)	1 (1)	1 (1)	1 (1)	1 (1)	1 (0)	0 (0)	0 (0)
% (± SD)		12 (12)	18 (28)	2 (4)	52 (25)	2 (4)	2 (4)	7 (10)	1 (3)	2 (3)	2 (7)	0 (0)	0 (0)
TRAP													
Upwelling													
10 ⁷ # m ⁻² d ⁻¹ (± SD)	591 (975)	0.2 (0.1)	1.1 (5.8)	0.7 (1.6)	0.5 (0.7)	0.1 (0.3)	5.3 (13)	40.3 (87.2)	23.0 (49.9)				
% (± SD)		2 (1)	6 (6)	2 (4)	2 (2)	1 (1)	14 (13)	46 (25)	20 (22)				
Downwelling													
10 ⁷ # m ⁻² d ⁻¹ (± SD)	2158 (4616)	0.2 (0.5)	0.9 (2.1)	9.2 (2.1)	1.3 (2.1)	0.3 (0.5)	31.2 (43.6)	25.6 (40.6)	43.9 (111)				
% (± SD)		1 (1)	1 (1)	2 (2)	3 (2)	1 (1)	23 (12)	28 (19)	24 (19)				
SEDIMENTS													
GeoB 11002-1													
10 ⁴ # valves gr ⁻¹	142	0	0	2	3	0	24	47	52				
%		0.2	0	2	2	0	17	33	37				
GeoB 11003-2													
10 ⁴ # valves gr ⁻¹	65	0	0	2	1	0	7	26	26				
%		1	0	3	2	0	10	39	39				



Figure captions

Fig. 1. Map of the NW Iberian Peninsula continental margin showing the position of the mooring line (RAIA) site. WANA hindcast reanalysis points 3027034 (WANA_S off Cape Silleiro) and 1044067 (WANA_G off A Guarda) from which wave data were obtained, location of the irradiance Cies station (IR) and positions of the sediment cores GeoB11002-1 and 5 GeoB11003-2 are also shown.

Fig. 2. Temporal series of (a) total irradiance at Cies station (IR), (b) upwelling index ($-Q_x$), (c) significant wave heights (Hs) obtained for propagation from the Silleiro and A Guarda WANA T points and, (d) Minho and Douro River discharges. Upwelling and downwelling periods are highlighted with white and grey bars, respectively, based on upwelling index and biogeochemical data presented in Zúñiga et al. (2016).

10 Fig. 3. Temporal series of (a) temperature (and water column integrated Brunt-Vaisälä frequency (N^2)), (b) nitrates (NO_3) and silicates ($\text{Si}(\text{OH})_4$) content and, (c) Chl *a* concentration and diatoms abundance measured at 5 m water depth. Upwelling and downwelling periods are highlighted with white and grey bars, respectively, based on upwelling index and biogeochemical data presented in Zúñiga et al. (2016).

Fig. 4. Time series of diatom abundances (a, c, e and g) and assemblages (b, d, f, h) at 5 m water depth. Water column 15 diatom species has been classified in order to easily compare them with fossil diatom assemblage from the sediment trap samples. *Nitzschia* spp: *Nitzschia longissima*; *Pseudo-nitzschia* spp: *Pseudo-nitzschia* cf. *delicatissima* and *Pseudo nitzschia* cf. *seriata*; Thal. nitzs: *Thalassionema nitzschioides*; small centric group: includes small centric diatoms and *Thalassiosira* spp. small; *Navicula* spp: *Navicula transitans* var. *derasa*; *Chaetoceros* (Ch.) spp: Ch. *curvisetus*, Ch. *socialis*, Ch. *didymus*, Ch. *lacinosus*, Ch. *decipiens* and small *Chaetoceros*; *Leptocylindrus* spp: *Leptocylindrus danicus*. Upwelling and 20 downwelling periods are highlighted with white and grey bars, respectively, based on upwelling index and biogeochemical data presented in Zúñiga et al. (2016).

Fig. 5. Time series of (a) biogenic silica (BioSi), (c) total siliceous organisms and (e) diatoms (including diatom valves and spores) fluxes registered at RAIA station. Relative contribution of (b) biogenic silica to total mass flux, (d) silicoflagellates 25 respect to total siliceous organisms and (f) resting spores to total diatoms flux are also presented. Upwelling and downwelling periods are highlighted with white and grey bars, respectively, based on upwelling index and biogeochemical data presented in Zúñiga et al. (2016).

Fig. 6. Time series of (a) benthic and (c) freshwater diatom fluxes (and relative contributions respect to total diatoms) (b, d) registered at RAIA station. Upwelling and downwelling periods are highlighted with white and grey bars, respectively, based on upwelling index and biogeochemical data presented in Zúñiga et al. (2016).

30 Fig. 7. Time series of marine diatoms fluxes (a, c, e) and assemblages (percentage respect to total marine diatoms) (b, d, f) registered at RAIA station. Fossil diatom species has been classified in three groups in order to compare them with water column diatom assemblage. *Nitzschia* spp: *Nitzschia marina*; *Pseudo-nitzschia* spp: *Pseudo-nitzschia pungens*; Thal. Nitzs: *Thalassionema nitzschioides*. Small centric group: includes *Coscinodiscus marginatus*, *Coscinodiscus radiatus* and



Thalassiosira eccentrica. Upwelling and downwelling periods are highlighted with white and grey bars, respectively, based on upwelling index and biogeochemical data presented in Zúñiga et al. (2016).

Fig. 8. RDA biplot results of the canonical ordination (only significant variables shown) for main fossil sediment trap diatom groups (freshwater (FW) diatoms, benthic diatoms, *Paralia sulcata* (Parsul), *Chaetoceros* spp. spores (ChaeRS) and
5 *Leptocylindrus* spp. spores (LepRS), and forward selected environmental variables (Chlorophyll *a* (Chl *a*), Temperature (Temp), nitrates (NO₃), silicates (Si(OH)₄) and Minho River flow). JFM: January-February-March, AMJ: April-May-June, JAS: July-August-September, OND: October-November-December.



Figure 1

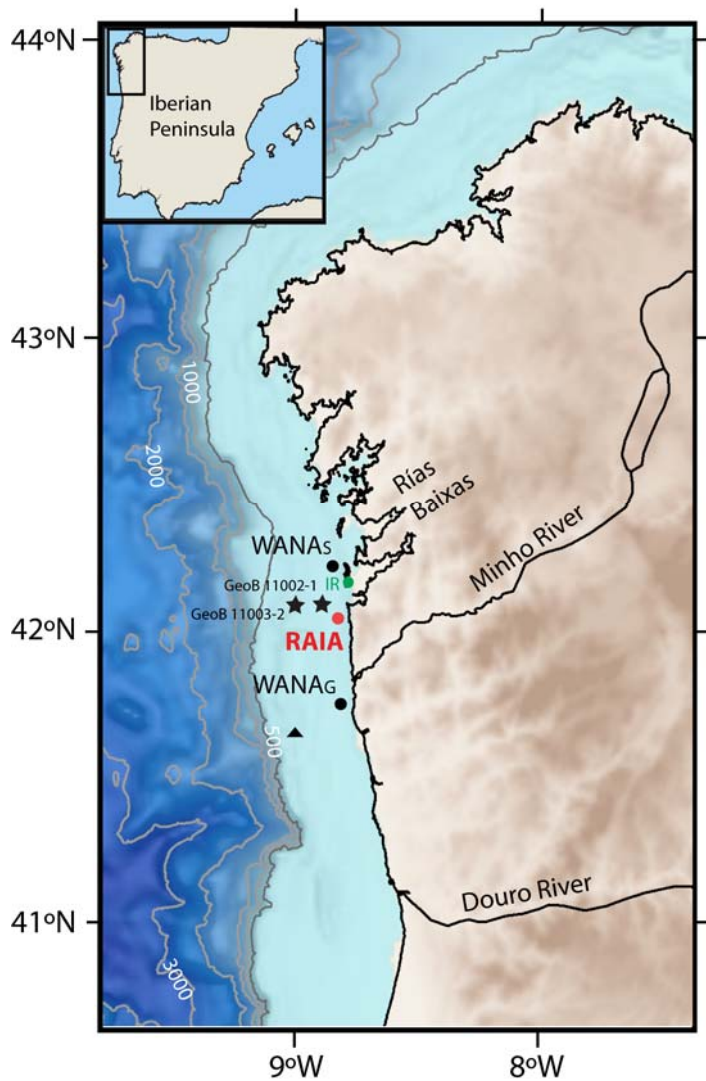




Figure 2

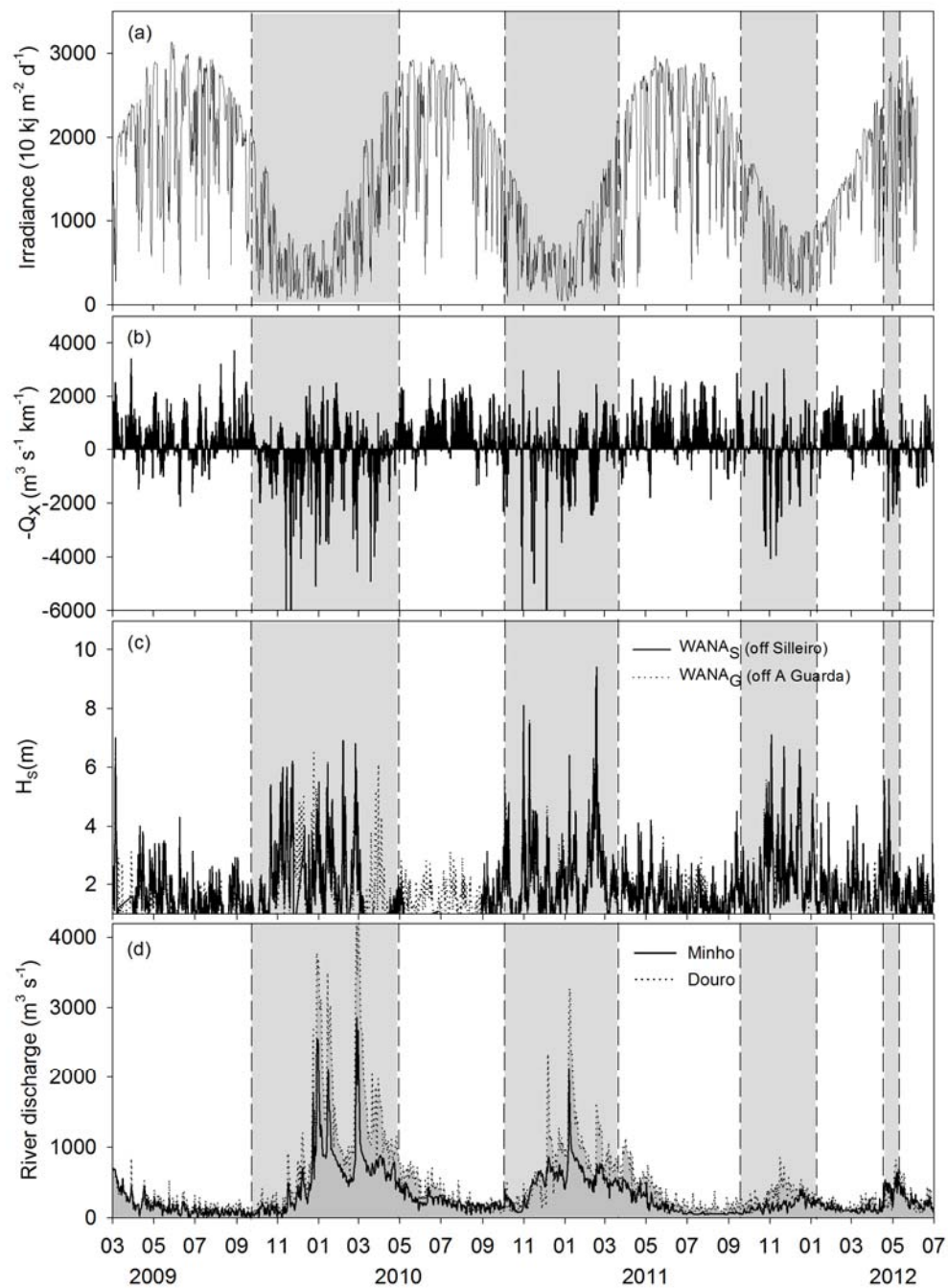




Figure 3

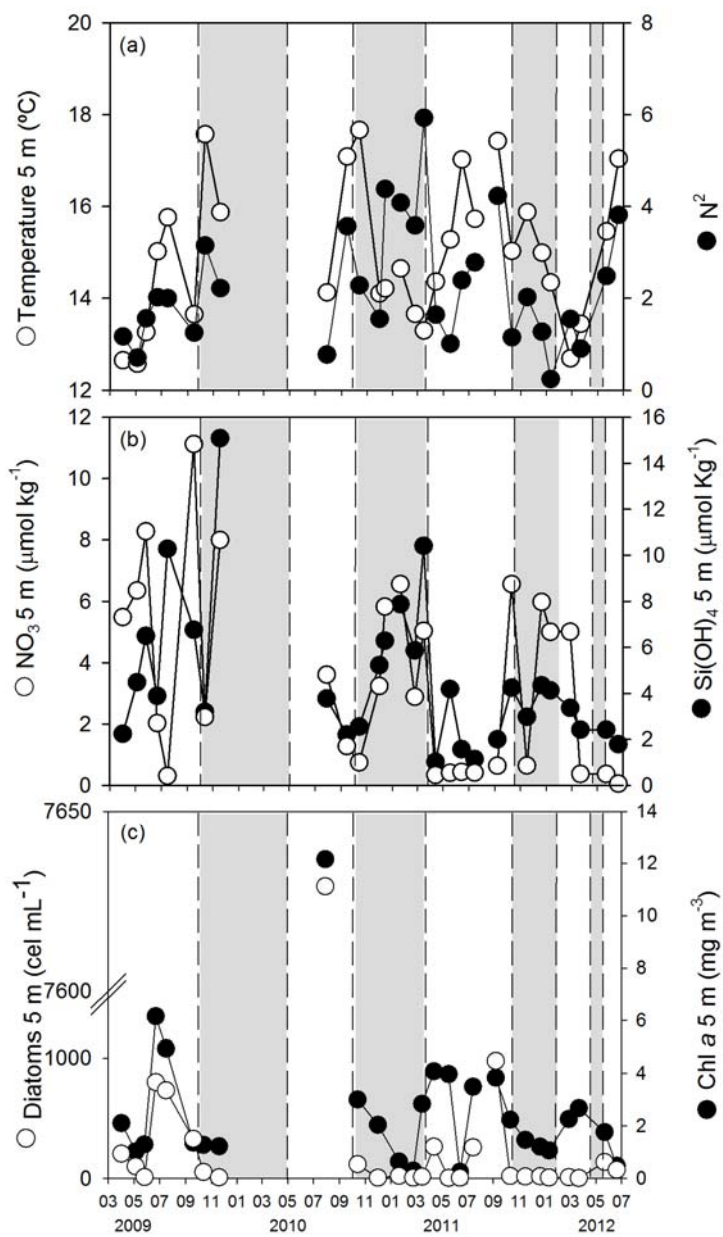


Figure 4

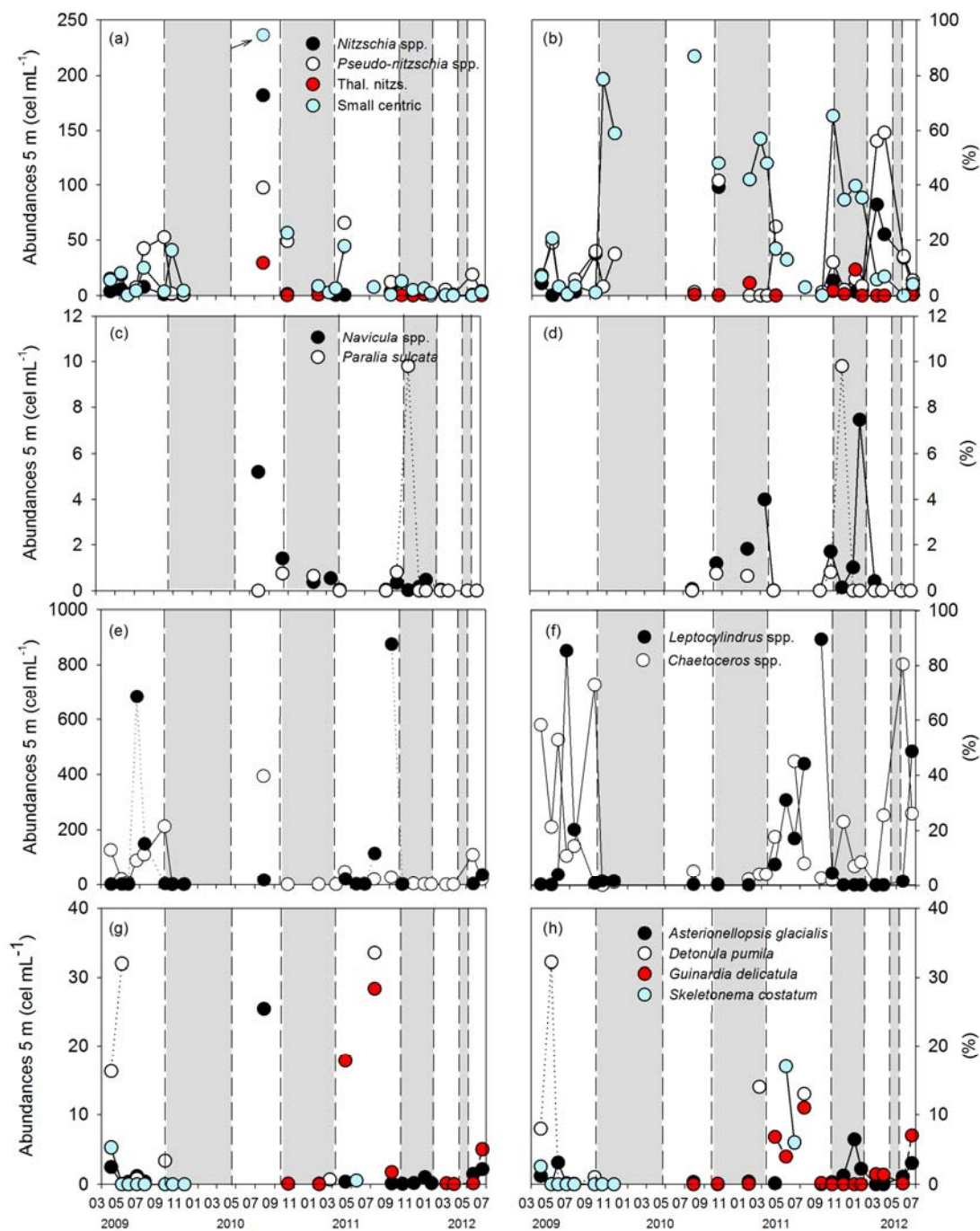




Figure 5

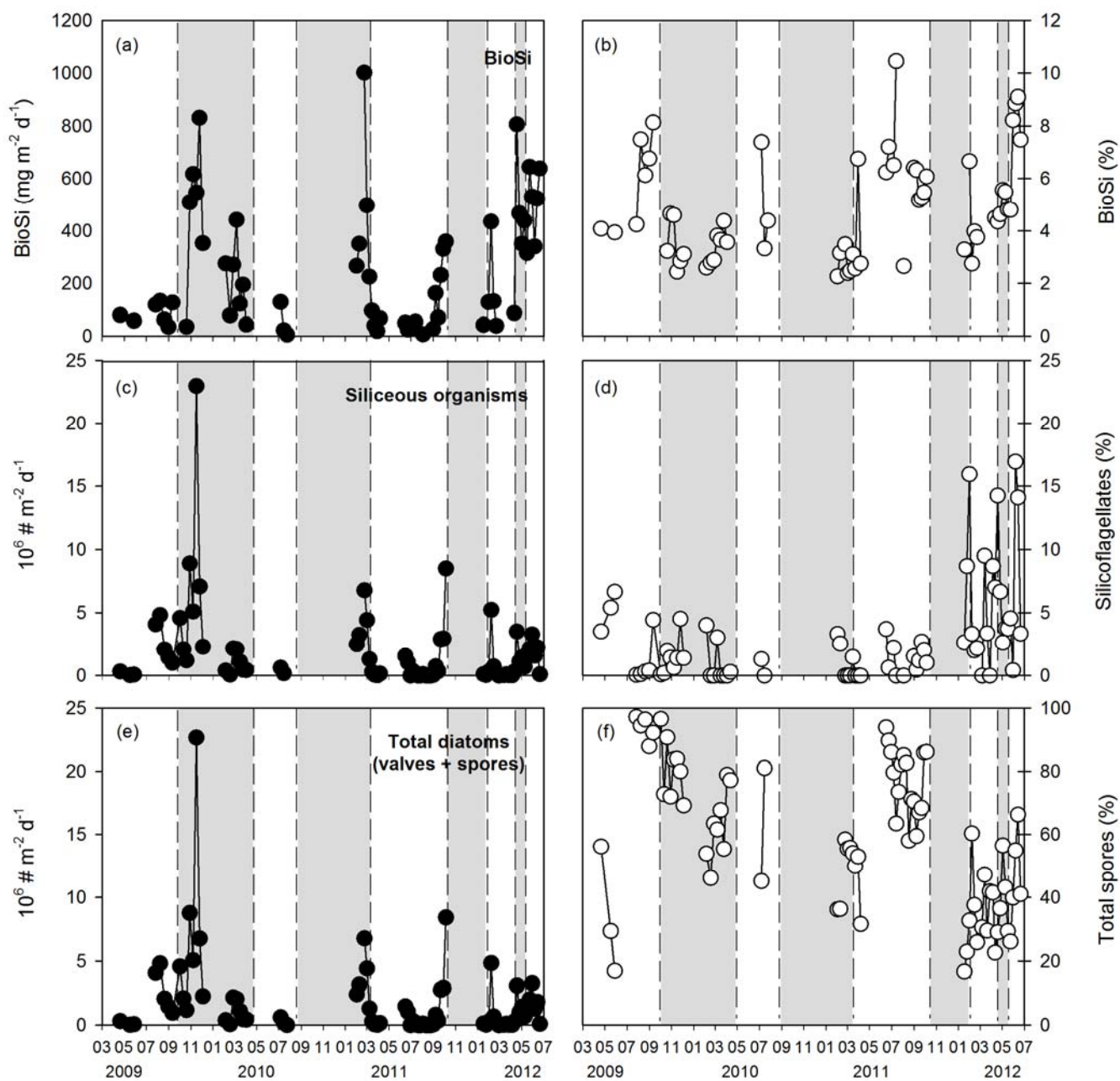
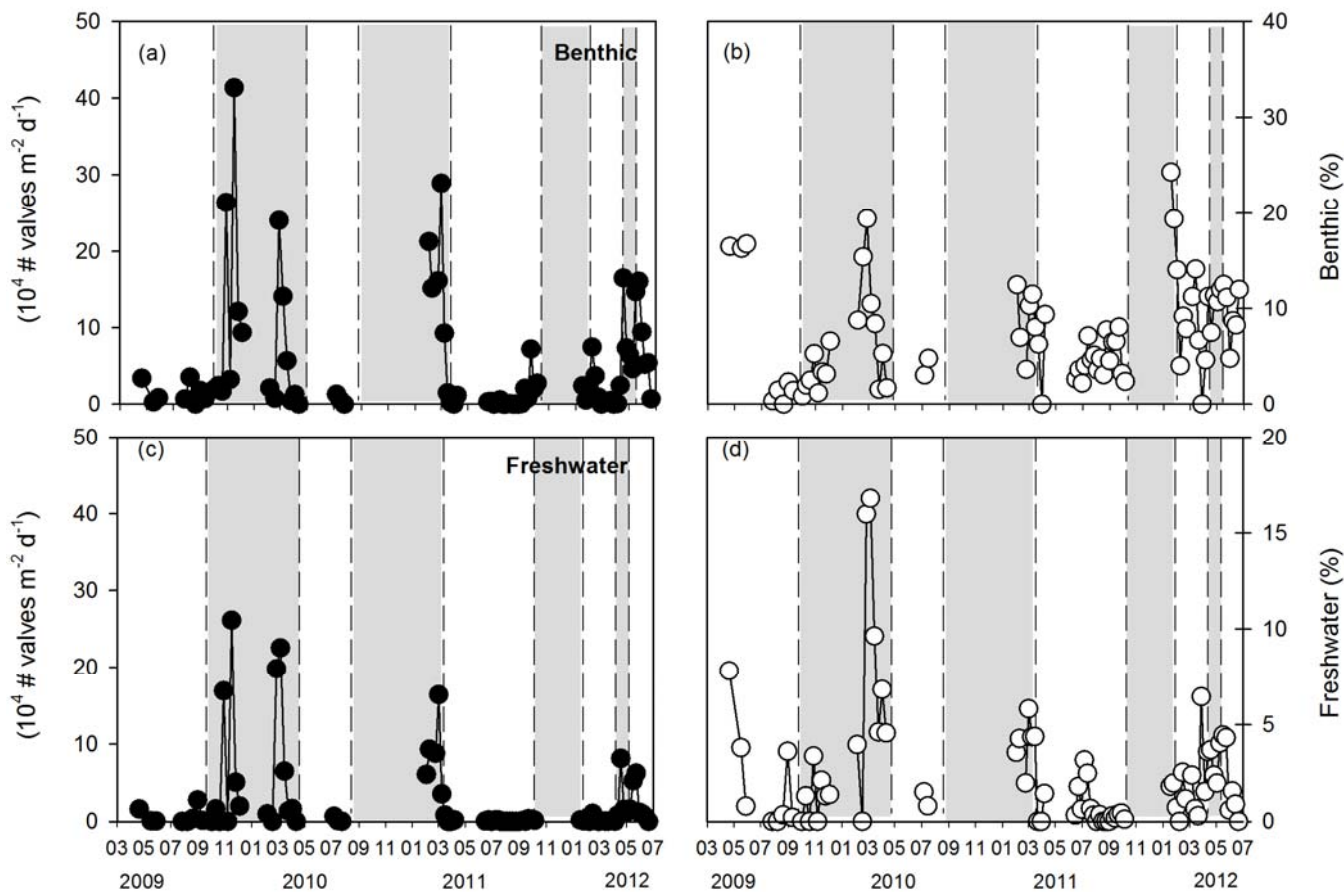




Figure 6



5

10



Figure 7

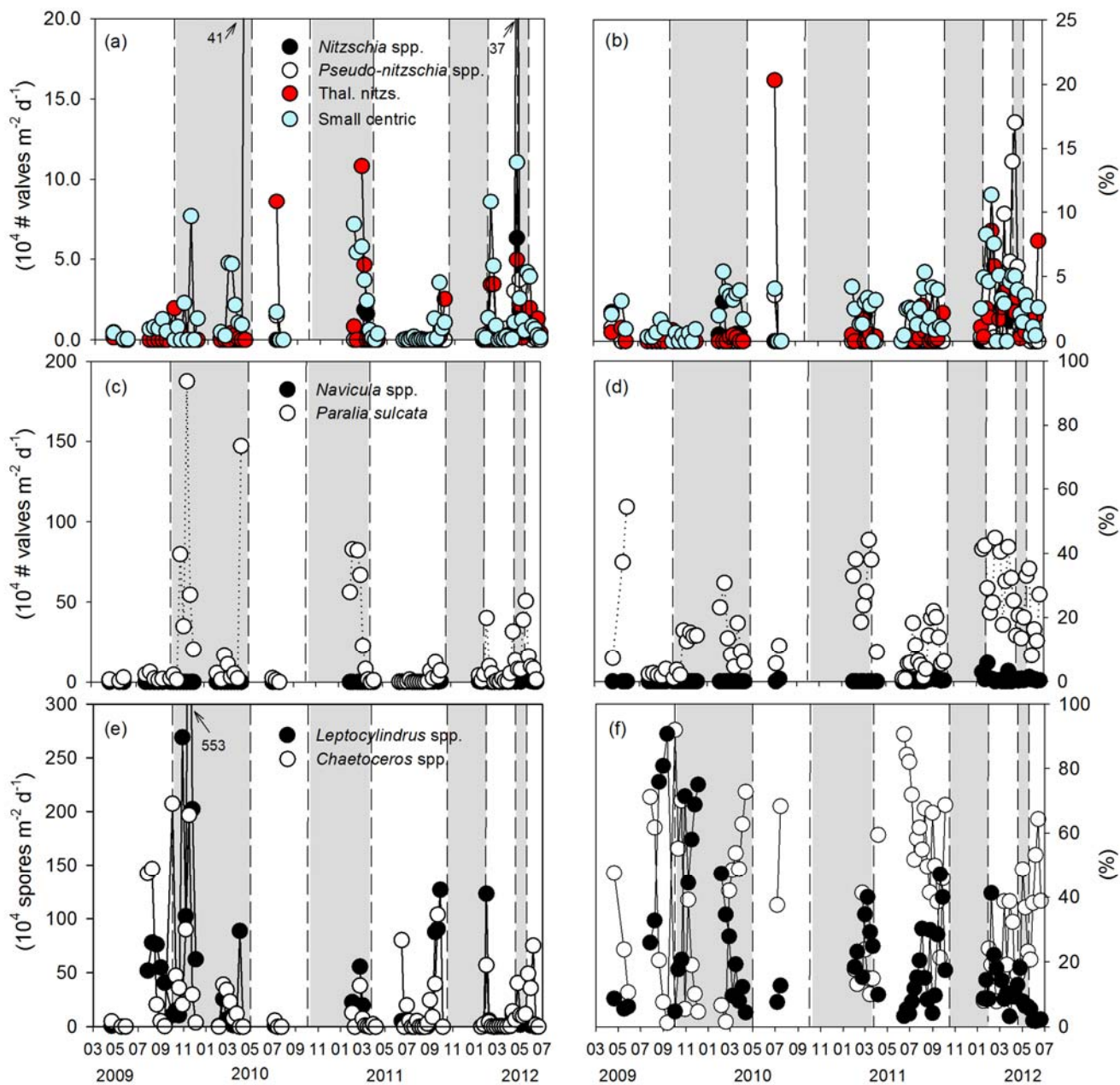
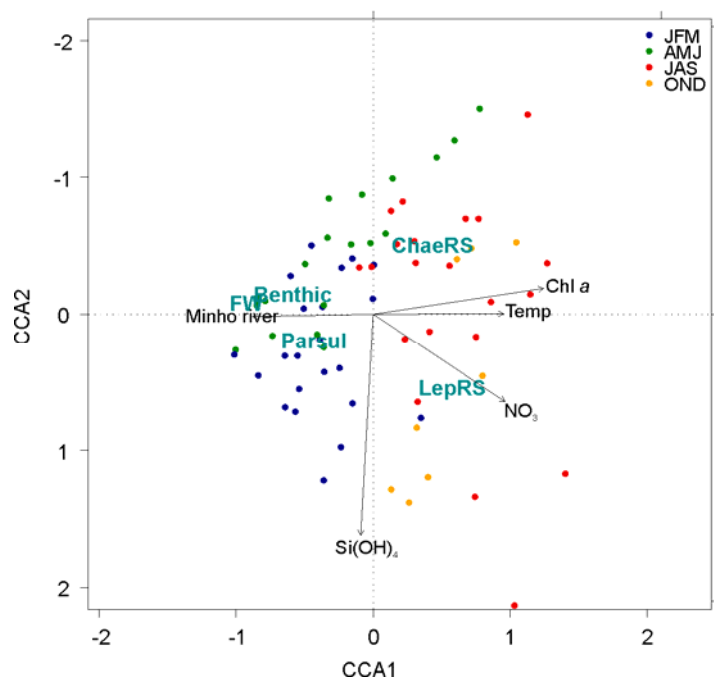




Figure 8



5

10

15

20



Appendix A. List of diatom species found in both the RAI A sediment trap and surficial sediment samples (Geo B 11002-1 and Geo 11003-2).

	Diatom species	Sediment trap	Sediments
5	<i>Achnanthes brevipes</i> C. Agardh	X	X
	<i>Achnanthes</i> sp.	X	
	<i>Actinocyclus curvatus</i> Janisch	X	X
	<i>Actinocyclus octonarius</i> Ehrenberg	X	
	<i>Actinocyclus</i> sp.	X	X
10	<i>Actinoptychus senarius</i> (Ehrenberg) Ehrenberg	X	X
	<i>Amphora gracilis</i> Ehrenberg	X	
	<i>Amphora marina</i> T.V. Desikachary & P. Prema	X	
	<i>Amphora</i> sp.	X	
	<i>Anorthoneis excentrica</i> (Donkin) Grunow	X	
15	<i>Asteromphalus flabellatus</i> (Brébisson) Greville	X	
	<i>Asteromphalus</i> sp.	X	
	<i>Aulacoseira</i> cf. <i>granulata</i> (Ehrenberg) Simonsen	X	X
	<i>Aulacoseira</i> sp.	X	X
	<i>Azpeitia neocrenulata</i> (S.L. VanLandingham)	X	
20	<i>Azpeitia nodulifera</i> (A. Schmidt) G.A. Fryxell & P.A. Sims	X	
	<i>Bacillaria paxillifera</i> (O.F. Müller) T. Marsson	X	
	<i>Bacteriastrium hyalinum</i> Lauder	X	
	<i>Caloneis</i> sp.	X	
	<i>Campylodiscus incertus</i> A.W.F. Schmidt	X	
25	<i>Campyloneis grevillei</i> (W. Smith) Grunow & Eulenstein	X	
	<i>Campylosira cymbelliformis</i> Grunow ex Van Heurck	X	
	<i>Cerataulus smithii</i> Ralfs ex Pritchard	X	
	<i>Chaetoceros lorenzianus</i> Grunow	X	
	<i>Chaetoceros</i> sp. (resting spores)	X	X
30	<i>Chaetoceros</i> sp.	X	
	<i>Cocconeis disculoides</i> (Hustedt) Stefano & Marino	X	
	<i>Cocconeis guttata</i> Husted & Aleem	X	
	<i>Cocconeis hoffmannii</i> Simonsen	X	
	<i>Cocconeis neodiminuta</i> Krammer	X	
35	<i>Cocconeis placentula</i> Ehrenberg	X	X
	<i>Cocconeis pseudomarginata</i> Gregory	X	
	<i>Cocconeis scutellum</i> Ehrenberg	X	X
	<i>Cocconeis speciosa</i> Gregory	X	
	<i>Cocconeis stauroneiformis</i> (W. Smith) H. Okuno	X	
40	<i>Cocconeis</i> sp.	X	
	<i>Coscinodiscus gigans</i> Ehrenberg	X	
	<i>Coscinodiscus marginatus</i> Ehrenberg	X	X
	<i>Coscinodiscus</i> cf. <i>oculus-iridis</i> (Ehrenberg) Ehrenberg	X	
	<i>Coscinodiscus radiatus</i> Ehrenberg	X	X
45	<i>Coscinodiscus</i> sp.	X	
	<i>Ctenophora pulchella</i> (Ralfs ex Kützing)	X	
	<i>Cyclotella meneghiniana</i> Kützing	X	X



	<i>Cyclotella plitvicensis</i> Husted	X	
	<i>Cyclotella stelligera</i> Cleve & Grunow in Van Heurck	X	
	<i>Cyclotella radiosa</i> (Grunow) Lemmermann	X	
	<i>Cyclotella</i> sp.	X	
5	<i>Cyclostephanos</i> sp.	X	
	<i>Cymbella affinis</i> Kützing	X	X
	<i>Cymbella</i> sp.	X	
	<i>Delphineis minutissima</i> (Husted) Simonsen	X	X
	<i>Delphineis surirella</i> (Ehrenberg) G.W. Andrews	X	
10	<i>Detonula pumila</i> (Castracane) Gran	X	
	<i>Dimeregramma minor</i> (Gregory) Ralfs ex Pritchard	X	
	<i>Diploneis</i> cf. <i>bombus</i> (Ehrenberg) Ehrenberg	X	X
	<i>Diploneis didymus</i> (Ehrenberg) Ehrenberg	X	
	<i>Diploneis smithii</i> (Brébisson) Cleve	X	
15	<i>Diploneis</i> cf. <i>stroemii</i> Husted	X	
	<i>Diploneis suborbicularis</i> (W.Gregory) Cleve	X	
	<i>Diploneis weissflogii</i> (A.W.F.Schmidt) Cleve	X	
	<i>Diploneis</i> sp.	X	
	<i>Dytilum</i> sp.	X	
20	<i>Encyonema</i> sp.	X	
	<i>Epithemia</i> sp.	X	
	<i>Eunotia</i> cf. <i>Pectinalis</i> (Kützing) Rabenhorst	X	
	<i>Eunotia praeurupta</i> (Grunow)	X	
	<i>Eunotia</i> sp.	X	
25	<i>Fragilariforma constricta</i> (Ehrenberg) D.M.Williams & Round	X	
	<i>Fragilaria crotonensis</i> (Kitton) Cleve & Möller	X	
	<i>Fragilaria inflata</i> (Heiden) Hustedt	X	
	<i>Fragilaria investiens</i> (W. Smith) Clever-Euler	X	
	<i>Fragilaria schulzii</i> Brockmann	X	
30	<i>Fragilaria ulna</i> (Nitzsch) Lange-Bertalot	X	X
	<i>Fragilaria</i> sp.	X	
	<i>Fragilariforma virescens</i> (Ralfs) D.M.Williams & Round	X	
	<i>Gomphonema</i> sp.	X	X
	<i>Gomphonema</i> cf. <i>acuminatum</i> (Ehrenberg)	X	
35	<i>Gomphonema</i> cf. <i>constrictum</i> (Ehrenberg)	X	
	<i>Gomphonema parvulum</i> (Kützing) Kützing	X	
	<i>Grammatophora angulosa</i> (Ehrenberg)	X	
	<i>Grammatophora marina</i> (Lyngbye) Kützing	X	X
	<i>Grammatophora oceánica</i> (Ehrenberg) Cleve	X	
40	<i>Grammatophora</i> sp.	X	
	<i>Grammatophora serpentina</i> (Ehrenberg) Hartley	X	
	<i>Haslea</i> sp.	X	
	<i>Hantzschia</i> sp.	X	
	<i>Hemidiscus cuneiformis</i> Wallich	X	
45	<i>Hemiaulus</i> sp.	X	
	<i>Hyalodiscus scoticus</i> (Kützing) Grunow	X	
	<i>Leptocylindrus</i> sp. (resting spores)	X	X
	<i>Licmophora abbreviata</i> (C.Agardh)	X	
	<i>Licmophora</i> sp.	X	
50	<i>Luticola mutica</i> (Kützing) D.G.Mann	X	



	<i>Lyrella</i> sp.	X	
	<i>Melosira moniliformis</i> (O.F.Müller) C.Agardh	X	
	<i>Melosira varians</i> C.Agardh	X	
	<i>Melosira westii</i> W. Smith	X	X
5	<i>Melosira</i> sp.	X	X
	<i>Navicula bacillum</i> Ehrenberg	X	
	<i>Navicula</i> cf. <i>cancellata</i> Donkin	X	
	<i>Navicula cincta</i> (Ehrenberg) Ralfs	X	
	<i>Navicula mutica</i> Kützing	X	
10	<i>Navicula</i> cf. <i>pennata</i> A.Schmidt	X	
	<i>Navicula</i> sp.	X	
	<i>Nitzschia angularis</i> W. Smith	X	
	<i>Nitzschia angustata</i> (W. Smith) Grunow	X	
	<i>Nitzschia longissima</i> (Brébisson) Ralfs	X	
15	<i>Nitzschia macilenta</i> W. Gregory	X	
	<i>Nitzschia marina</i> Grunow	X	X
	<i>Nitzschia panduriformis</i> W. Gregory	X	
	<i>Nitzschia umbonata</i> (Ehrenberg) H. Lange-Bertalot	X	
	<i>Nitzschia</i> sp.	X	X
20	<i>Odontella aurita</i> (Lyngbye) C.Agardh	X	
	<i>Odontella longicruris</i> (Greville) M.A.Hoban	X	
	<i>Odontella</i> sp.	X	
	<i>Opephora marina</i> (W. Gregory) Petit	X	
	<i>Opephora martyi</i> Héribaud	X	X
25	<i>Opephora</i> sp.	X	
	<i>Paralia sulcata</i> (Ehrenberg) Cleve	X	X
	<i>Petronis humerosa</i> (Brébisson ex W.Smith) Stickle & D.G.Mann	X	
	<i>Pinnularia borealis</i> Ehrenberg	X	
	<i>Pinnularia</i> sp.	X	
30	<i>Pleurosigma elongatum</i> W. Smith	X	
	<i>Pleurosigma normanii</i> Ralfs in Pritchard	X	
	<i>Pleurosigma</i> sp.	X	
	<i>Pleurosira laevis</i> (Ehrenberg) Compère	X	
	<i>Porosira glacialis</i> (Grunow) Jørgensen	X	
35	<i>Podosira stelliger</i> (Bailey) Mann	X	X
	<i>Proboscia alata</i> (Brightwell) Sundström	X	
	<i>Psammodiscus nitidus</i> (Gregory) Round & Mann	X	
	<i>Pseudo-nitzschia pungens</i> (Grunow ex Cleve) G.R.Hasle	X	
	<i>Pseudo-nitzschia seriata</i> (Cleve) H.Peragallo	X	
40	<i>Raphoneis ampiceros</i> (Ehrenberg) Ehrenberg	X	
	<i>Rhabdonema arcuatum</i> (Lyngbye) Kützing	X	
	<i>Rhabdonema minutum</i> Kützing	X	
	<i>Rhabdonema</i> sp.	X	
	<i>Rhizosolenia bergonii</i> Peragallo	X	
45	<i>Rhizosolenia hebetata</i> (Bailey) Gran	X	
	<i>Rhizosolenia</i> sp.	X	
	<i>Rhoicosphenia abbreviata</i> (C.Agardh) Lange-Bertalot	X	
	<i>Rhoicosphenia marina</i> (Kützing) M.Schmidt	X	
	<i>Roperia tessellata</i> (Roper) Grunow ex Pelletan	X	X
50	<i>Staurisirella pinnata</i> (Ehrenberg) D.M.Williams & Round	X	



	<i>Staurosirella</i> sp.	X	
	<i>Stellarima stellaris</i> (Roper) G.R.Hasle & P.A.Sims	X	
	<i>Stephanodiscus astrea</i> (Ehrenberg) Grunow	X	
	<i>Stephanodiscus</i> sp.	X	X
5	<i>Stephanopyxis turris</i> (Greville) Ralfs in Pritchard	X	
	<i>Surirella</i> sp.	X	
	<i>Synedra gaillonii</i> (Bory) Ehrenberg	X	
	<i>Synedra</i> sp.	X	
	<i>Tabellaria fenestrata</i> (Lyngbye) Kützing	X	
10	<i>Tabellaria flocculosa</i> (Roth) Kützing	X	
	<i>Tabellaria</i> sp.	X	
	<i>Tetracyclus glans</i> (Ehrenberg) F.W.Mills	X	
	<i>Thalassiosira eccentrica</i> (Ehrenberg) Cleve	X	X
	<i>Thalassiosira cf. leptopus</i> (Grunow) Hasle & G.Fryxell	X	X
15	<i>Thalassiosira lineata</i> Jousé	X	
	<i>Thalassiosira</i> sp.	X	X
	<i>Thalassionema nitzschioides</i> (Grunow) Mereschkowsky	X	X
	<i>Toxarium undulatum</i> Bailey	X	
	<i>Trachyneis aspera</i> (Ehrenberg) Cleve 1894	X	X
20	<i>Triceratium favus</i> Ehrenberg	X	
	<i>Tryblionella navicularis</i> (Brébisson) Ralfs	X	